Backward probability model using multiple observations of contamination to identify groundwater contamination sources at the Massachusetts Military Reservation

R. M. Neupauer[1]

Department of Civil Engineering, University of Virginia, Charlottesville, Virginia, USA

J. L. Wilson

Department of Earth and Environmental Science, New Mexico Institute of Mining and Technology, Socorro, New Mexico, USA

Received 22 December 2003; revised 28 November 2004; accepted 7 December 2004; published 12 February 2005.

[1] Backward location and travel time probability density functions characterize the possible former locations (or the source location) of contamination that is observed in an aquifer. For an observed contaminant particle the backward location probability density function (PDF) describes its position at a fixed time prior to sampling, and the backward travel time probability density function describes the amount of time required for the particle to travel to the sampling location from a fixed upgradient position. The backward probability model has been developed for a single observation of contamination (e.g., Neupauer and Wilson, 1999). In practical situations, contamination is sampled at multiple locations and times, and these additional data provide information that can be used to better characterize the former position of contamination. Through Bayes' theorem we combine the individual PDFs for each observation to obtain a PDF for multiple observations that describes the possible source locations or release times of all observed contaminant particles, assuming they originated from the same instantaneous point source. We show that the multiple-observation probability density function is the normalized product of the single-observation PDFs. The additional information available from multiple observations reduces the variances of the source location and travel time probability density functions and improves the characterization of the contamination source. We apply the backward probability model to a trichloroethylene (TCE) plume at the Massachusetts Military Reservation (MMR). We use four TCE samples distributed throughout the plume to obtain single-observation and multiple-observation location and travel time PDFs in three dimensions. These PDFs provide information about the possible sources of contamination. Under assumptions that the existing MMR model is properly calibrated and the conceptual model is correct the results confirm the two suspected sources of contamination and reveal that one or more additional sources is likely.

Citation: Neupauer, R. M., and J. L. Wilson (2005), Backward probability model using multiple observations of contamination to identify groundwater contamination sources at the Massachusetts Military Reservation, *Water Resour. Res.*, *41*, W02015, doi:10.1029/2003WR002974.

1. Introduction

[2] Backward-in-time modeling can be used to identify source locations or former positions of contamination that is observed in an aquifer. The results of a backward-in-time model are backward location and travel time probability density functions. The backward location probability density function (PDF) describes the possible former positions of the observed contamination at a fixed time in the past, and the backward travel time probability density function describes the possible travel times of the contaminant from a selected upgradient position to the observation location. *Neupauer and Wilson* [1999, 2001] showed that backward PDFs are related to adjoint states of concentration, and they presented a formal framework for obtaining the governing equation of the backward model using adjoint theory. In the adjoint model, an instantaneous point source of an adjoint state (related to the PDFs) is released at the observation location at the time of observation. The adjoint state is transported upgradient and backward-in-time, following all fate and transport processes (including dispersion) that occur in forward contaminant transport modeling. The resulting spatial distribution at a point in time is related to

[1]Now at Department of Civil, Environmental and Architectural Engineering, University of Colorado, Boulder, Colorado, USA.

0043-1397/05/2003WR002974$09.00

the backward location PDF describing the possible former and source locations of the observed contamination. Similarly, a breakthrough curve at a fixed point in space is related to the backward travel time PDF describing possible travel times and, if the point is a candidate source location, possible release times. With one simulation of the backward model, information is obtained about all possible sources for one observation. The backward model has been developed for conservative solutes in steady flow fields [*Neupauer and Wilson*, 1999, 2001], for transport in nonuniform and transient flow fields [*Neupauer and Wilson*, 2002], and for reactive transport including first-order decay [*Neupauer and Wilson*, 2003] and linear equilibrium and nonequilibrium sorption [*Neupauer and Wilson*, 2004b]. The approach was used by *Fogg et al.* [1999] to assess vulnerability of groundwater to nitrate contamination in the Salinas Valley, California, and by *Weissmann et al.* [2002] to evaluate groundwater ages in the Kings River Alluvial Fan near Fresno, California. *Michalak and Kitanidis* [2004] coupled this adjoint method with a geostatistical approach to reconstruct historical distributions of groundwater contamination.

[3] The backward model can also be used to delineate a probabilistic capture zone for a water supply pumping well. A probabilistic capture zone is a map showing the probability that contamination from any upgradient position will reach the well within a specified time; therefore it represents many possible source locations and one observation location (the well). It is the spatial distribution of a cumulative distribution function of forward travel time and can be obtained with one simulation of a backward probability model. *Uffink* [1989] and *Chin and Chittaluru* [1994] used a backward random walk approach to delineate probabilistic capture zones around pumping wells. *Frind et al.* [2002] used the adjoint method to delineate a capture zone for Greenbrook municipal water supply well field in the Waterloo moraine, while *Neupauer and Wilson* [2004a] use the method to delineate aquifer remediation capture zones at the Massachusetts Military Reservation.

[4] Backward probability models have been developed for single observations of contamination; however, in practical situations, multiple samples of contamination are often taken over both space and time. This additional information improves the characterization of the former position of the observed contamination through a variance reduction of the backward probability density functions. The purpose of this paper is to extend the single-observation backward probability model to multiple observations of contamination. When contamination is observed in an aquifer, the concentration is generally known; however, in this paper, we deal only with the presence or absence of contamination, and not with the actual measured values. We treat each observation as a contaminant "particle", similar to fluid particles used in classical transport theory [e.g., *Taylor*, 1921; *Saffman*, 1959; *Dagan*, 1987] that provides the foundation for the concept of dispersion. The particle is transported through the aquifer as a unit. At any time, it exists either entirely in the aqueous phase or entirely in the sorbed phase, and the mass of the particle does not change during transport. Although we ignore the measured concentrations in this paper, the results from the present work will form the foundation of an approach for conditioning the backward probability density functions on measured concentrations, which is the subject of a future paper. Even in the absence of measured concentrations, the use of multiple observations in the backward model substantially reduces the range of possible former or source locations.

[5] The multiple-observation probability model is related to the two-particle stochastic model of forward contaminant transport, which frequently uses a stochastic representation of the heterogeneous hydraulic conductivity field. If two particles originate from the same source, they initially follow similar travel paths. Their separation distance is small and their positions are correlated. This early time behavior of a pair of particles, characterized by a small separation distance, is analogous to a compact contaminant plume with a small dispersion coefficient. As their travel distance increases, each particle follows a different travel path, and therefore the particles sample different heterogeneities, resulting in less correlation in their positions and a growing dispersion coefficient. As the particles eventually sample all or most of the heterogeneities, the particle positions become less correlated, and the dispersion coefficient approaches an asymptotic value. Expressions for this scale-dependent dispersion coefficient have been developed based on velocity variations and covariances between particle pairs [e.g., *Kitanidis*, 1988; *Dagan*, 1990, 1991; *Salandin et al.*, 1991; *Rajaram and Gelhar*, 1993a, 1993b; *Zhang et al.*, 1996]. Although it is now well known that dispersion is scale-dependent, most standard contaminant transport codes, such as MT3DMS [*Zheng and Wang*, 1999], solve the advection-dispersion equation with a constant (i.e., independent of travel distance) dispersion coefficient. Use of standard codes therefore assumes that a sufficient amount of time has passed such that the particle positions are uncorrelated, and the assumption of an asymptotic (constant value) dispersion coefficient is valid. We make this assumption here.

[6] In the next section, we review the backward probability model for a single observation of contamination, and we develop the new backward location and travel time probability density functions using multiple observations of contamination. Using a hypothetical example, we show that the variances of the multiple-observation PDFs are smaller than the variances of the single-observation PDFs. Next we demonstrate the use of the new technique on a trichloroethylene plume at the Massachusetts Military Reservation on Cape Cod to discern the likelihood that the source of contamination was one of two suspected sources. Finally we discuss some important features of the multiple-observation backward probability model.

2. Backward Probability Model

[7] Backward location and travel time probability density functions for a single observation of contamination are obtained by solving the adjoint of a forward contaminant transport equation. When multiple observations of contamination are made, a multiple-observation location or travel time PDF can be obtained by first calculating the single-observation PDFs for each observation, and then combining them to form a multiple-observation probability density function. In this section, we briefly summarize the procedure for obtaining single-observation PDFs. Using Bayes' theorem and probability theory, we

develop an expression for the multiple-observation PDFs based on single-observation PDFs. We present a simple example to illustrate some important features of the multiple-observation probability model.

2.1. Single-Observation Probability Density Functions

[8] The governing equation for the backward probability model is the adjoint of the governing equation of forward solute transport. Solute transport in groundwater can be modeled using the advection-dispersion-reaction equation (ADE)

$$R\theta\frac{\partial C}{\partial t} = \frac{\partial}{\partial x_i}\left(D_{ij}\theta\frac{\partial C}{\partial x_j}\right) - \frac{\partial}{\partial x_i}(v_i\theta C) - \theta\lambda C + q_I C_I - q_O C, \quad (1)$$

$$C(\mathbf{x},0) = C_i(\mathbf{x})$$

$$C(\mathbf{x},t) = g_1(t) \text{ on } \Gamma_1$$

$$\left[D_{ij}\frac{\partial C}{\partial x_j}\right]\mathrm{n}_i = g_2(t) \text{ on } \Gamma_2$$

$$\left[v_i C - D_{ij}\frac{\partial C}{\partial x_j}\right]\mathrm{n}_i = g_3(t) \text{ on } \Gamma_3$$

accounting for advection, dispersion, linear equilibrium sorption, and first-order decay, where $C(\mathbf{x}, t)$ is resident concentration, t is time, x_i are the spatial directions (i = 1, 2, 3), $\mathbf{x} = (x_1, x_2, x_3)$, D_{ij} is the i, jth entry of the dispersion tensor, v_i is the groundwater velocity in the direction of x_i, R is the retardation coefficient, θ is porosity, λ is the first-order decay rate, q_I is the source flow rate per unit volume, C_I is the source strength, q_O is the sink flow rate per unit volume, C_i is the initial concentration, g_1, g_2, and g_3 are known functions, Γ_1, Γ_2, and Γ_3 are the domain boundaries, and n_i is the outward unit normal vector in the x_i direction. The mathematical model for backward PDFs for a single observation of contamination is the adjoint of (1), given by [*Neupauer and Wilson*, 2002, 2003, 2004b]

$$R\theta\frac{\partial \psi^*}{\partial \tau} = \frac{\partial}{\partial x_i}\left(D_{ij}\theta\frac{\partial \psi^*}{\partial x_j}\right) + \frac{\partial}{\partial x_i}(v_i\theta\psi^*) - \theta\lambda\psi^* - q_I\psi^* + \frac{\partial h}{\partial C} \quad (2)$$

$$\psi^*(\mathbf{x},0) = 0$$

$$\psi^*(\mathbf{x},\tau) = 0 \text{ on } \Gamma_1$$

$$\left[D_{ij}\frac{\partial \psi^*}{\partial x_j} + v_i\psi^*\right]\mathrm{n}_i = 0 \text{ on } \Gamma_2$$

$$\left[D_{ij}\frac{\partial \psi^*}{\partial x_j}\right]\mathrm{n}_i = 0 \text{ on } \Gamma_3.$$

where ψ^* is the adjoint state (related to either the location or travel time PDF), τ is backward time or time prior to sampling ($\tau = t_o - t$, where $t = t_o$ is an arbitrary time usually taken as the time of the most recent observation), and h is a performance functional that depends on the type of probability. The load term $\partial h/\partial C$ is a Frèchet derivative of the performance functional, h, with respect to concentration, C [*Neupauer and Wilson*, 1999].

[9] The adjoint equation (2) has the same form as (1), except that the flow field is reversed, the time derivative is in terms of backward time, and the boundary conditions are slightly modified (second type boundaries in (1) become third type boundaries in (2) and vice versa). To calculate the backward location PDF for a contaminant particle observed at location $\mathbf{x}_w$ at backward time τ_w, (2) is solved with a performance functional of $h = C\delta(\mathbf{x} - \mathbf{x}_w)\delta(\tau - \tau_w)$, and the resulting adjoint state is related to the backward location PDF using [*Neupauer and Wilson*, 2002]

$$f_{\mathbf{X}}(\mathbf{x};\tau,\mathbf{x}_w,\tau_w) = \theta(\mathbf{x})\psi^*(\mathbf{x},\tau), \quad (3)$$

where $f_{\mathbf{X}}(\mathbf{x};\tau,\mathbf{x}_w,\tau_w)$ represents the probability density that a contaminant particle that was observed at location $\mathbf{x}_w$ at backward time τ_w was at random location $\mathbf{X}$ at time τ prior to observation (deterministic parameter). In this probability notation, variables to the right of the semicolon are deterministic parameters, and variables to the left of the semicolon are random variables. Here, the observation location and time ($\mathbf{x}_w$ and τ_w, respectively) and the backward time of interest (τ) are all deterministic parameters; while the former position $\mathbf{X}$ is the only random variable. The backward location probability density function in (3) defines an ensemble of possible prior positions of the observed contaminant particle.

[10] To calculate the travel time probability density function, (2) is solved with a performance functional of $h = C^f\delta(\mathbf{x} - \mathbf{x}_w)\delta(\tau - \tau_w)$ [*Neupauer and Wilson*, 2001], where C^f is flux concentration, and the adjoint state is related to the backward travel time PDF using [*Neupauer and Wilson*, 2002]

$$f_T(\tau;\mathbf{x},\mathbf{x}_w,\tau_w) = |v(\mathbf{x})|\theta(\mathbf{x})A(\mathbf{x})\psi^*(\mathbf{x},\tau), \quad (4)$$

where $f_T(\tau;\ \mathbf{x},\ \mathbf{x}_w,\ \tau_w)$ is the probability density that a contaminant particle that was observed at location $\mathbf{x}_w$ and time $\tau = \tau_w$ was at deterministic position $\mathbf{x}$ at random backward time T, $A(\mathbf{x})$ is the area of a plane perpendicular to the flow field across which the travel time PDF is desired, and vertical bars denote magnitude. Following the probability notation described above, the observation location and time ($\mathbf{x}_w$ and τ_w, respectively) and the former position ($\mathbf{x}$) are deterministic parameters, and the backward time T is a random variable. The backward travel time probability density in (4) defines an ensemble of possible travel times from location $\mathbf{x}$ to the observation location $\mathbf{x}_w$, to be observed at backward time $\tau = \tau_w$.

[11] The term $-q_I\psi^*$ in (2) represents the adjoint of the inflow of contamination through internal sources. If the inflow concentration is negligible ($C_I \approx 0$), the internal source term $+q_I C_I$ in (1) vanishes, and its adjoint term, $-q_I\psi^*$ in (2) also vanishes (see *Neupauer and Wilson* [2002] for a complete derivation). For example, the internal source term in (1) can represent an inflow of contamination with natural recharge. If the concentration of the contaminant in the recharge water is negligible, the internal source term $+q_I C_I$ in (1) vanishes, and consequently, its adjoint $-q_I\psi^*$ in (2) also vanishes.

[12] For a solute that undergoes first-order decay, two different interpretations of backward probability density are possible [*Neupauer and Wilson*, 2003]. The first interpretation accounts for the probability that the observed contaminant particle could have decayed prior to its being observed. With this interpretation, the backward PDFs are

obtained directly from (2), (3), and (4), which allows the adjoint state to decay. The resulting probability density functions show that distant sources and long travel times are less likely because contamination from these sources is likely to have decayed before reaching the observation location. In the second interpretation, the probability density functions are conditioned on the fact that the observed contaminant particle itself did not decay. The conditioned PDFs are obtained by normalizing the PDFs in (3) and (4) by either the total mass of contaminant in the aquifer at time τ (for location PDF) or the total mass of contaminant that passes location $\mathbf{x}$ (for travel time PDF). Additional details about these two interpretations are given by *Neupauer and Wilson* [2003].

[13] For sorbing solutes the source can be in either the aqueous phase or the sorbed phase. The location PDF in (3) represents the probability density that the observed contaminant particle was in the aqueous phase at random location $\mathbf{X}$ at time τ in the past (deterministic parameter). The probability density that the observed contaminant particle was in the sorbed phase at random location $\mathbf{X}$ at time τ in the past, $f^S_{\mathbf{X}}(\mathbf{x}; \tau, \mathbf{x}_w, \tau_w)$, is given by [*Neupauer and Wilson*, 2004b]

$$f^S_{\mathbf{X}}(\mathbf{x}; \tau, \mathbf{x}_w, \tau_w) = [R(\mathbf{x}) - 1] f_{\mathbf{X}}(\mathbf{x}; \tau, \mathbf{x}_w, \tau_w). \tag{5}$$

Likewise, the travel time PDF in (4) represents the probability density that the observed contaminant particle was released from location $\mathbf{x}$ (deterministic parameter) in the aqueous phase at random time T in the past. The probability density that the observed contaminant particle was released from the sorbed phase at location $\mathbf{x}$ at random time T in the past, $f^S_T(\tau; \mathbf{x}, \mathbf{x}_w, \tau_w)$, is given by

$$f^S_T(\tau; \mathbf{x}, \mathbf{x}_w, \tau_w) = \frac{R(\mathbf{x}) - 1}{R(\mathbf{x})} f_T(\tau; \mathbf{x}, \mathbf{x}_w, \tau_w). \tag{6}$$

2.2. Multiple-Observation Probability Density Functions

[14] When multiple observations of contamination are made, either at multiple locations, at multiple times, or both, each observation provides additional information that can be used to characterize the former position of contamination, thus reducing the uncertainty or variance of the location or travel time PDFs. In this section, we develop new multiple-observation location and travel time probability density functions. We ignore the measured concentrations and only consider whether or not contamination is present at the observation locations. In our derivation, we assume that the observed contaminant particles originated from the same location at the same time, implying that the source of contamination was an instantaneous point source. If all observed contaminant particles originated from the same instantaneous point source at backward time τ, the former positions of the particles would have coincided at backward time τ. The derived multiple-observation backward location PDF therefore describes the probability density that the observed contaminant particles were all at random location $\mathbf{X}$ at deterministic time τ in the past, given that their positions coincided at backward time τ. That is, $\mathbf{X}$ represents the point source location if the source release occurred at backward time τ. The multiple-observation backward travel time PDF describes the probability density that the observed contaminant particles were all at deterministic location $\mathbf{x}$ at random time T in the past, given that they were all present at that location at the same time. That is, T represents the instantaneous source release time.

[15] Let us define the joint density function of the random former positions of N observed contaminant particles as

$$f_{\mathbf{X}_1,\mathbf{X}_2,\ldots,\mathbf{X}_N}(\mathbf{x}_1, \mathbf{x}_2, \ldots, \mathbf{x}_N; \tau, \{\mathbf{x}_w\}, \{\tau_w\})$$

where $\mathbf{X}_i$ is the random former position of the ith observed contaminant particle at backward time τ; $\mathbf{x}_i$ is the particular former position of the ith observed contaminant particle; $\{\mathbf{x}_w\}$ is a vector of N observation locations, $\mathbf{x}_{wi}$; and $\{\tau_w\}$ is a vector of N observation times, τ_{wi}, in backward time. Once again, all variables to the right of the semicolon are deterministic. For the multiple-observation backward location PDF, we assume that all observed particles were at the same location $\mathbf{x}$ at backward time τ (i.e., the observed particles originated from a single instantaneous point source), therefore we can condition the joint density on the event, E, that $\mathbf{x}_1 = \mathbf{x}_2 = \ldots = \mathbf{x}_N = \mathbf{x}$ as

$$f_{\mathbf{X}_1,\mathbf{X}_2,\ldots,\mathbf{X}_N|E}(\mathbf{x}, \mathbf{x}, \ldots, \mathbf{x}|E; \tau, \{\mathbf{x}_w\}, \{\tau_w\}).$$

This is the probability density function that we are ultimately seeking. It describes the possible former location of the N particles at time τ in the past, given the event that all N particles were at the same location (e.g., the instantaneous point source location) at that time. Since all N particles were at the same location, let us define $\mathbf{X}$ as the single random source location (the same $\mathbf{X}$ for all particles). The conditioned backward PDF can now be defined as

$$f_{\mathbf{X}_1,\mathbf{X}_2,\ldots,\mathbf{X}_N|E}(\mathbf{x}, \mathbf{x}, \ldots, \mathbf{x}|E; \tau, \{\mathbf{x}_w\}, \{\tau_w\}) = f_{\mathbf{X}}(\mathbf{x}; \tau, \{\mathbf{x}_w\}, \{\tau_w\}), \tag{7}$$

where $f_{\mathbf{X}}(\mathbf{x}; \tau, \{\mathbf{x}_w\}, \{\tau_w\})$ is the probability density function describing the random source location of the contamination, assuming that the N contaminant particles were observed at locations $\{\mathbf{x}_w\}$ at backward times $\{\tau_w\}$, respectively, and that the instantaneous source release occurred at backward time τ.

[16] The probability expressed in (7) is related to the N single-observation location PDFs (one for each observation) through Bayes' theorem for mixed continuous and discrete probabilities which is given by

$$f_{\mathbf{X}_1,\mathbf{X}_2,\ldots,\mathbf{X}_N|E}(\mathbf{x}, \mathbf{x}, \ldots, \mathbf{x}|E; \tau, \{\mathbf{x}_w\}, \{\tau_w\}) = \frac{P(E|\mathbf{X}_1 = \mathbf{x}, \mathbf{X}_2 = \mathbf{x}, \ldots, \mathbf{X}_N = \mathbf{x}; \tau) f_{\mathbf{X}_1,\mathbf{X}_2,\ldots,\mathbf{X}_N}(\mathbf{x}, \mathbf{x}, \ldots, \mathbf{x}; \tau)}{\int P(E|\mathbf{X}_1 = \mathbf{x}, \mathbf{X}_2 = \mathbf{x}, \ldots, \mathbf{X}_N = \mathbf{x}; \tau) f_{\mathbf{X}_1,\mathbf{X}_2,\ldots,\mathbf{X}_N}(\mathbf{x}, \mathbf{x}, \ldots, \mathbf{x}; \tau) d\mathbf{x}}, \tag{8}$$

where we dropped the vectors of observation locations and times on the right-hand side to simplify the notation. The first probability in both the numerator and denominator is a discrete probability that is either equal to one or zero

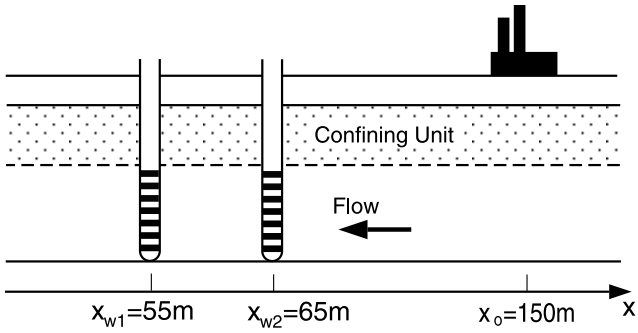

Figure 1. Sample one-dimensional aquifer.

depending on the conditioning statement. Since the probability is conditioned on each particle's being at the same $\mathbf{x}$, then event E, that all particles are at the same location, must be true; therefore the discrete probability in both the numerator and denominator is equal to one. With the assumption that the random particle positions are uncorrelated (asymptotic value of the dispersion coefficient is valid), the joint probability density function, $f_{\mathbf{X}_1,\mathbf{X}_2,\ldots,\mathbf{X}_N}(\mathbf{x}, \mathbf{x},\ldots, \mathbf{x}; \tau)$, can be separated into the product of the PDFs of the individual components of $\{\mathbf{X}\}$, each given by $f_{\mathbf{X}}(\mathbf{x}; \tau, \mathbf{x}_{wi}, \tau_{wi})$, the single-observation location PDF for observation i, given in (3). Making these substitutions and using (7), we obtain the final expression for the N-observation location PDF

$$f_{\mathbf{X}}(\mathbf{x}; \tau, \{\mathbf{x}_w\}, \{\tau_w\}) = \frac{\prod_{i=1}^{N} f_{\mathbf{X}}(\mathbf{x}; \tau, \mathbf{x}_{wi}, \tau_{wi})}{\int \prod_{i=1}^{N} f_{\mathbf{X}}(\mathbf{x}; \tau, \mathbf{x}_{wi}, \tau_{wi})\, d\mathbf{x}}, \qquad (9)$$

where $f_{\mathbf{x}}(\mathbf{x}; \tau, \{\mathbf{x}_w\}, \{\tau_w\})$ represents the probability density of the random position $\mathbf{X}$ of all N observed particles at backward time τ, given the N observation locations $\{\mathbf{x}_w\}$ and N observation times $\{\tau_w\}$, and given that the position of all N particles coincided at backward time τ. Following the same approach for travel time, we obtain the N-observation travel time PDF, given by

$$f_T(\tau; \mathbf{x}, \{\mathbf{x}_w\}, \{\tau_w\}) = \frac{\prod_{i=1}^{N} f_T(\tau; \mathbf{x}, \mathbf{x}_{wi}, \tau_{wi})}{\int \prod_{i=1}^{N} f_T(\tau; \mathbf{x}, \mathbf{x}_{wi}, \tau_{wi})\, d\tau}. \qquad (10)$$

where $f_T(\tau; \mathbf{x}, \mathbf{x}_{wi}, \tau_{wi})$ is the single-observation travel time PDF for observation i given in (4), and $f_T(\tau; \mathbf{x}, \{\mathbf{x}_w\}, \{\tau_w\})$ is the probability density of the random backward time T at which all N observed particles were at location $\mathbf{x}$, given the N observation locations $\{\mathbf{x}_w\}$ and N observation times $\{\tau_w\}$, and given that all particles were at $\mathbf{x}$ at the same time.

[17] The procedure for numerically calculating the multiple-observation location probability density function is to first run one backward location probability simulation for each of the N observations to obtain N single-observation location PDFs. These single-observation location PDFs are used in (9) to obtain the multiple-observation location PDF. If the probability density functions are obtained through numerical simulations using finite difference methods or other discrete approximations, then the spatial discretization must be consistent for all simulations. In such a discretized solution, (9) can be solved by finding the product of the values of the N single-observation PDFs at each node on the numerical grid, and normalizing the result by its integral over the spatial domain.

[18] To calculate the multiple-observation travel time probability density function, one backward travel time probability simulation must be run for each of the N observations. The resulting single-observation travel time PDFs are used in (10) to obtain the multiple-observation travel time PDF. Again, if the PDFs are obtained through a numerical discretization method, the temporal discretization must be consistent for all simulations, and the simulations must be of sufficient duration so that the tails of the travel time PDFs are essentially complete. Using such a discretized solution, (10) can be solved by finding the product of the values of the N single-observation PDFs at each time step, and normalizing the result by its integral over the temporal domain.

[19] In practice, simulation methods are almost always used. Since it is necessary, in general, to run one backward simulation for each observation, the procedure may become computationally inefficient if a large number of observations are considered. The numerical implementation of the single-observation backward probability model is described by *Neupauer and Wilson* [2004a].

[20] Unlike single-observation probability density functions, the multiple-observation location and travel time PDFs always integrate to unity over the spatial and temporal domains, respectively. The integral of a single-observation travel time PDF over backward time represents the probability that the observed contaminant particle was ever at the location of interest [*Neupauer and Wilson*, 2001]. This information cannot be obtained from the multiple-observation PDFs because they are conditioned on the observed particles' having been at the location of interest, and therefore integrate to unity. The integral of a single-observation location PDFs represents the probability that the contaminant particle was anywhere in the aquifer at the time of interest. Under certain conditions, such as internal fluid sources [see *Neupauer and Wilson*, 2002] and reactive solutes [see *Neupauer and Wilson*, 2003, 2004b], the particle might not have been in the aquifer at the time of interest, or may have been present in a different phase (e.g., aqueous or sorbed). Again, this information cannot be obtained from the multiple-observation location PDF because it is conditioned on the particles' having been in the aquifer at the time of interest, and therefore integrates to unity.

2.3. Example

[21] As an example of the multiple-observation probability model, consider the one-dimensional confined aquifer in Figure 1. Flow is from right to left in Figure 1, and transport parameters are shown in Table 1. If contamination is released instantaneously from a source at x_o = 150 m, the resulting

Table 1. Transport Parameter Values for the One-Dimensional Example

Parameter	Value
Dispersion coefficient D	3 m^2/d
Velocity v	−1 m/d
Observation location (particle 1) x_{w1}	55 m
Observation location (particle 2) x_{w2}	65 m
Observation time (particle 1) τ_{w1}	0
Observation time (particle 2) τ_{w2}	20 days

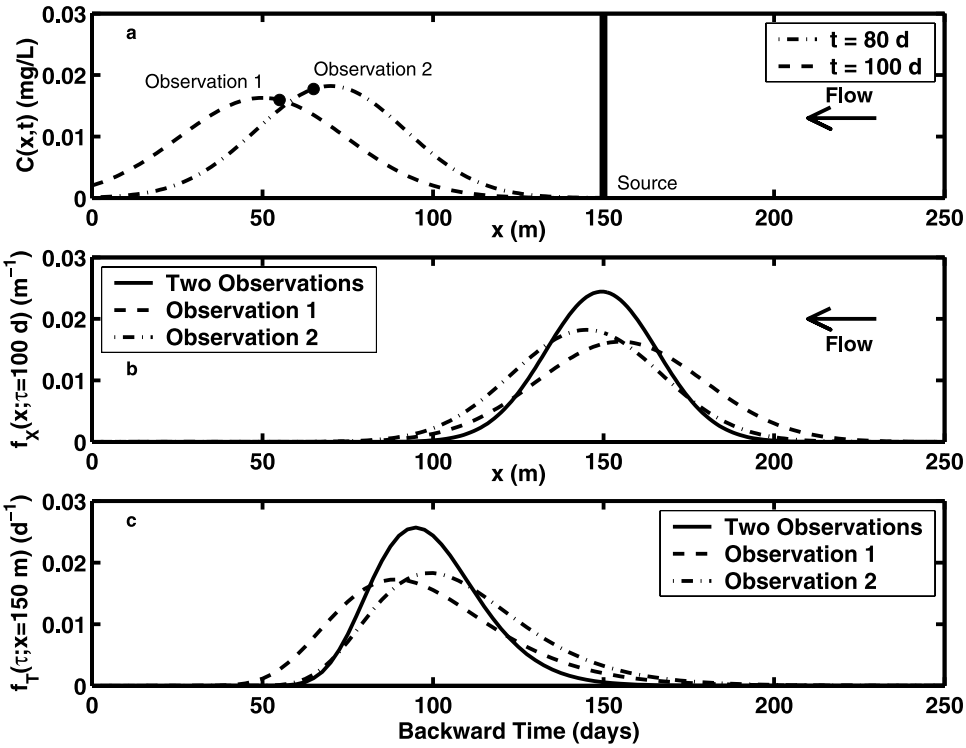

Figure 2. Results of the one-dimensional example. (a) Concentration in the aquifer after release of contamination from an instantaneous point source at x = 150 m. Circles represent samples used in the backward model. (b) Backward location probability density function at τ = 100 days. (c) Backward travel time probability density function at x = 150 m. Particle 1 was observed at location x_{w1} = 55 m at time τ_{w1} = 0, and particle 2 was observed at location x_{w2} = 65 m at time τ_{w2} = 20 days. (D = 3 m^2/d, v = −1 m/d).

concentration distributions at t = 80 days and t = 100 days after release are shown in Figure 2a. Suppose contamination is observed at location x_{w1} = 55 m at the present time (t = 100 days; τ_{w1} = 0) (observation 1), and contamination was observed 20 days ago (t = 80 days; τ_{w2} = 20 days) at location x_{w2} = 65 m (observation 2), as shown by the circles in Figure 2a. We calculated the single-observation and two-observation location PDFs at τ = 100 days in the past (100 days prior to sampling at x_{w1}), and the single-observation and two-observation travel time PDFs at x = 150 m. The results are shown in Figures 2b and 2c, respectively.

[22] Considering each observation separately, the likely former positions of the two observed contaminant particles are represented by the single-observation backward location probability density functions. The most likely position of observation 1 (dashed line in Figure 2b) at backward time τ = 100 days is $x \approx 154$ m; while the most likely position of observation 2 (dot-dashed line in Figure 2b) at the same backward time is $x \approx 144$ m. Assuming both observed contaminant particles were released from the same location at τ = 100 days, the likely source location is described by the two-observation backward location PDF (solid line in Figure 2b), and the most likely source location is $x \approx 149$ m.

[23] The likely individual travel times of the two observed particles from an assumed source at x = 150 m are represented by the single-observation backward travel time PDFs. The most likely travel time for observation 1 (dashed line in Figure 2c) is $\tau \approx 90$ days; while the most like travel time for observation 2 (dot-dashed line in Figure 2c) is $\tau \approx 100$ days. Assuming both observed contaminant particles were released at the same time from location x = 150 m, the likely travel time (or release time) is shown in the two-observation backward travel time PDF (solid line in Figure 2c), which shows the most likely release time of $\tau \approx 95$ days.

[24] Table 2 shows that the variances of the two-observation PDFs are significantly smaller than the variances of the single-observation PDFs. Even though the measured concentration values themselves were not used, the additional information obtained from the multiple observations reduces the uncertainty of the results, and this is quantified by a variance reduction.

3. Identification of a TCE Source at the Massachusetts Military Reservation

[25] In this section, we demonstrate the use of the multiple-observation backward probability model in a field application. Since the purpose of this section is to demonstrate the modeling approach, we have chosen to use an existing, published model. *Zheng and Wang* [2002] devel-

Table 2. Variances of the Single- and Two-Observation Probability Density Functions for the One-Dimensional Example

	Variance	
Observation	Location PDF, m^2	Travel Time PDF, days^2
Observation 1	600	614
Observation 2	480	554
Two observations	267	261

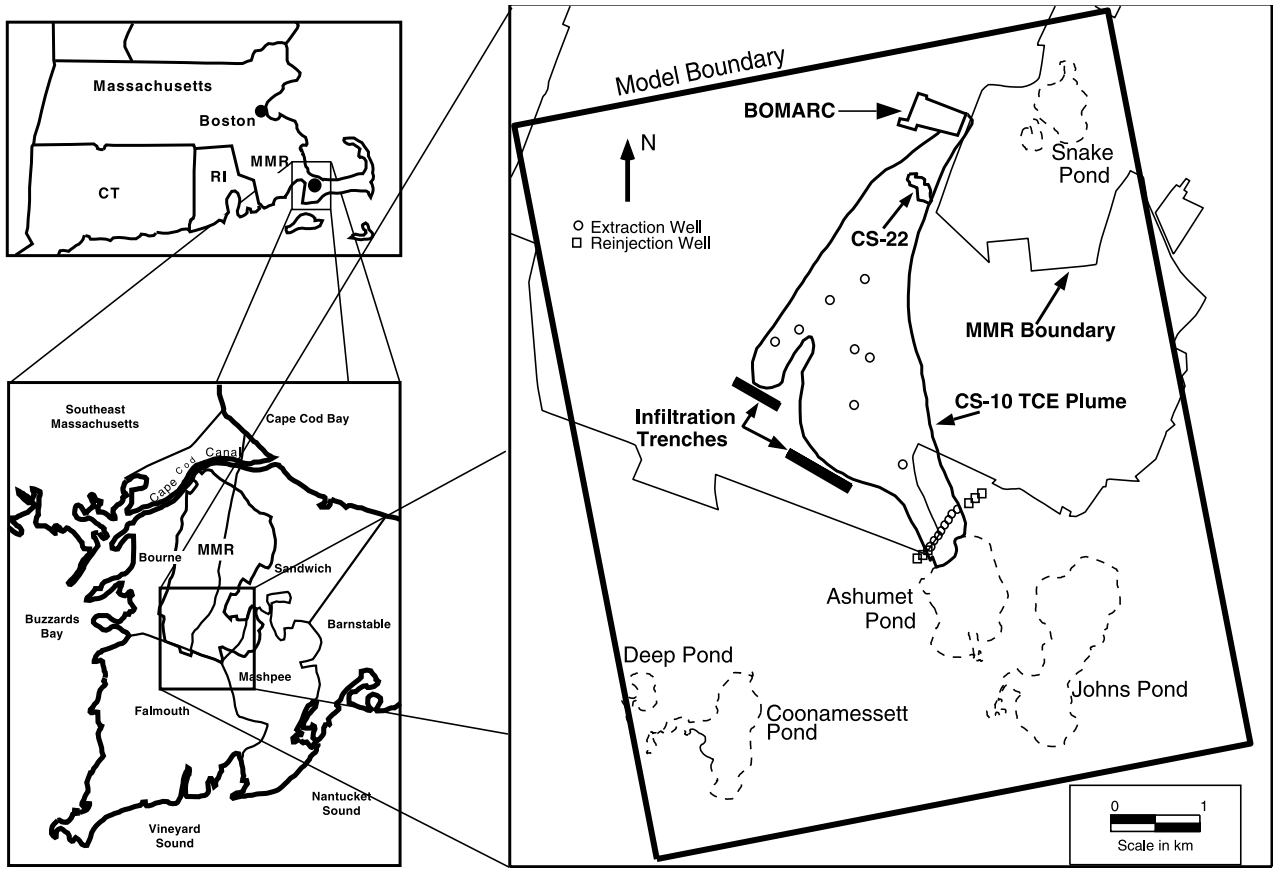

Figure 3. Location of Massachusetts Military Reservation (MMR), the inferred CS-10 plume (5 μg/L contour in 1997), the possible sources areas, the remediation system, and the model domain boundary. Adapted from *AFCEE* [1998, 1999].

oped a flow and transport model to optimize the design of the remediation system for a trichloroethylene (TCE) contaminated site at the Massachusetts Military Reservation (MMR). Using their model as the foundation for our backward probability model, we demonstrate the use of the multiple-observation backward probability model to identify possible sources of TCE.

[26] As with all models, the MMR TCE model is a simplification of reality and may have conceptual, parametric, and numerical flaws. For examples of each, consider that the model assumes equilibrium sorption, assumes spatially uniform dispersivity and retardation values, and has sufficiently large grid blocks to cause numerical dispersion. Our results therefore should be viewed as an illustration of the backward modeling procedure and the type of information that can be obtained from it. Further validation and sensitivity analysis of the MMR model would be needed in order to use the results as conclusive evidence of source locations.

[27] In this section, we first provide a brief description of the site and MMR model. Additional information is given by *Zheng and Wang* [2002]. Next we demonstrate the use of the multiple-observation backward probability model for identifying possible sources of the TCE.

3.1. CS-10 Site Description

[28] Massachusetts Military Reservation (MMR) is a military training facility covering approximately 89 km^2 on the western edge of Cape Cod in Massachusetts (see Figure 3). MMR is situated over the recharge area of the Sagamore Lens, a 90-m-thick sand aquifer that is the sole-source aquifer supplying drinking water for western Cape Cod. In 1989 the U.S. Environmental Protection Agency (USEPA) added MMR to the National Priorities List because of several groundwater plumes and soil contamination that could potentially contaminate the drinking water supply [*USEPA*, 1991]. This study addresses the Chemical Spill 10 (CS-10) plume, a TCE plume in the southeast corner of the MMR (see Figure 3). The plume is approximately 5 km (17,000 feet) long, 2 km (6000 feet) wide, and up to 43 m (140 feet) thick. It is over 37 m (120 feet) below ground surface and 18 m (60 feet) below the water table along most of its length [*Zheng and Wang*, 2002]. The maximum TCE concentration sampled between 1996 and 2000 was 5110 μg/L, sampled near Ashumet Pond in June 1997. This concentration is significantly higher than the primary drinking water standard of 0.005 ppm (≈5 μg/L) (U.S. Environmental Protection Agency, Code of Federal Regulations, 40 CFR 141.61, Maximum contaminant levels for organic contaminant, Washington, D. C., 1 July 1999).

[29] A suspected source area for the CS-10 plume is the former Boeing Michigan Aerospace Research Center (BOMARC) Missile Site, near the eastern boundary of the MMR (see Figure 3), which was in operation between 1962 and 1973. The area is presently used for maintenance and storage of vehicles. Spills and releases of chemicals occurred

Table 3. Transport Parameter Values for the MMR TCE Simulations[a]

Parameter	Value
Porosity	0.3
Longitudinal dispersivity	11 m (35 feet)
Horizontal transverse dispersivity	1.1 m (3.5 feet)
Vertical transverse dispersivity	0.11 m (0.35 feet)
Retardation coefficient	1.56
First-order decay rate	3.16×10^{-5} d^{-1}

[a]From *Zheng and Wang* [2002].

in this area in the past. Another possible source area is CS-22 (see Figure 3) where unspecified waste, possibly from the BOMARC facility, may have been disposed [*Air Force Center for Environmental Excellence* (*AFCEE*), 2000]. To remediate the CS-10 plume, contaminated groundwater is extracted through 16 extraction wells, is treated, and reenters the aquifer through six reinjection wells and two infiltration trenches (see Figure 3) [*Zheng and Wang*, 2002].

3.2. CS-10 Flow and Transport Model

[30] *Zheng and Wang* [2002] simulated flow and transport of the CS-10 TCE plume under remediation conditions using MODFLOW-96 [*Harbaugh and McDonald*, 1996] and MT3DMS [*Zheng and Wang*, 1999]. The model domain is a 6840 m × 8450 m (22,440 feet × 27,720 feet) rectangular region, discretized into 159 columns, 161 rows, and 21 layers (see Figure 3). The horizontal spatial discretization ranges from 34 m (110 feet) near the plume to 200 m (660 feet) near the boundaries. Vertical thickness of layers ranges from less than 1.5 m (5 feet) to over 15 m (50 feet) [*Zheng and Wang*, 2002].

[31] The boundary conditions for the flow model are specified flux at the top of the upper layer with recharge rates ranging from 41 to 86 cm/yr (16 to 34 in/yr), no flow at the bottom of the lowest layer, and specified head at the side boundaries, with values interpolated from a regional flow model created by Jacobs Engineering Group [*Zheng and Wang*, 2002]. Hydraulic conductivity in the model domain ranges from 3 m/d (10 feet/d) for silts to over 91 m/d (300 feet/d) for coarse sands. The average hydraulic gradient is approximately 0.001. Groundwater velocity ranges from 0.3 m/d (1 feet/d) to more than 1.2 m/d (4 feet/d), generally in the south-southwest direction, and flow is essentially horizontal [*Zheng and Wang*, 2002].

[32] The boundary conditions for the transport model are zero gradient at all boundaries (i.e., no dispersive flux). The forward transport model of *Zheng and Wang* [2002] modeled the physical processes of advection and dispersion, and the chemical processes of linear equilibrium sorption of TCE and first-order decay of TCE, presumably due to biotic and abiotic dechlorination processes. See Table 3 for additional parameter values. Although the flow model included natural recharge, the concentration of TCE in the recharge water was assumed to be negligible. We assume that the model of *Zheng and Wang* [2002] is correctly calibrated for both flow and transport parameter values, and using it we apply the backward modeling approach to identify possible TCE sources.

3.3. CS-10 Backward Probability Model

[33] The backward probability model is obtained by solving the adjoint equation (2), which has a reversed flow field relative to the forward contaminant transport model (1). Since we are interested in the former position of the TCE, we used a preremediation flow field. We assumed steady flow, and we used the flow model of *Zheng and Wang* [2002] but eliminated the remediation extraction wells, injection wells, and infiltration trenches from the simulation (see Figure 3). The resulting forward groundwater flow field is illustrated by the water table elevations in Figure 4. The hydraulic head distribution is essentially unchanged over the depth of the model. For the backward probability model, we reversed this flow field using a procedure described by *Neupauer and Wilson* [2004a].

[34] The initial condition of the backward model is homogeneous everywhere ($\psi^* = 0$). All boundary conditions are third-type (zero flux), consistent with the zero-gradient boundary conditions in the forward model (compare the boundary conditions on Γ_2 in (1) and (2)). We used the same transport processes and parameters as *Zheng and Wang* [2002] used in their forward model (see Table 3). Because $C_I = 0$ in the forward model, we eliminated the recharge term $-q_I\psi^*$ from (2) to solve the backward model. In addition, we used the second interpretation for decay, i.e., we conditioned the PDFs on the fact the the observed contaminant particles did not decay. We solved the backward model using MT3DMS (version 3.50.B), using the implicit finite difference method with upstream weighting of the advective term, and using the generalized conjugate gradient matrix solver with the SSOR preconditioner.

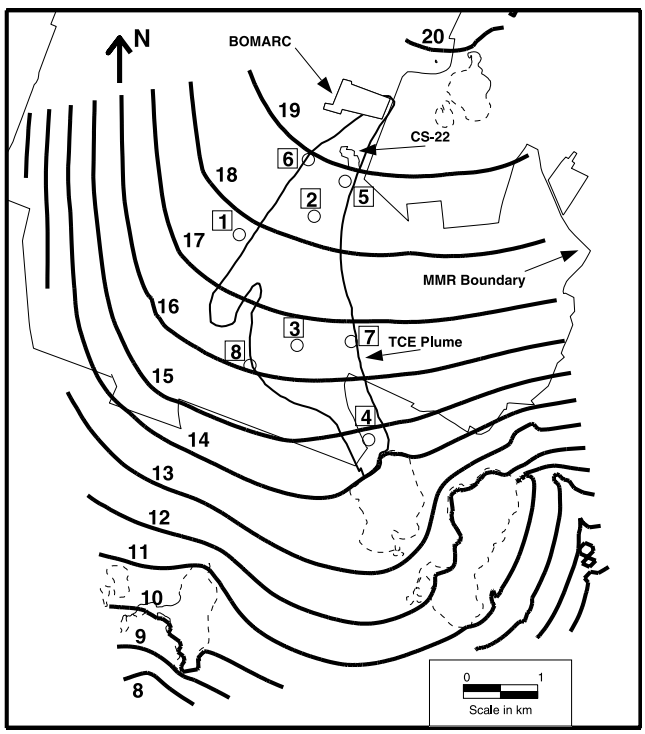

Figure 4. Water table elevations at MMR from the forward flow simulation (units are m). The circles denote sample locations. The boxed numbers denote the sample number.

Table 4. TCE Samples Used in the Backward Model

Sample	Sample Date	Concentration, μg/L
1	11 Sept. 1996	58
2	21 June 2000	150
3	26 Oct. 1998	203.1
4	13 June 1997	5110
5	22 Oct. 1996	12
6	30 Oct. 1996	2.2
7	29 Sept. 1998	170
8	21 May 1997	0.6

[35] Of the hundreds of samples of TCE taken throughout the plume area between 1996 and 2000, we selected four samples (numbered 1 through 4; see Table 4 and Figure 4) to use in the backward model. Sample 1, from a shallow monitoring well, is the earliest sample available; sample 2 is the most recent sample available at the time of the simulations, and is taken from an intermediate depth near the center of the plume; sample 3 is in the center of the plume at an intermediate depth; and sample 4 is from a deep monitoring well and has the highest concentration of the samples taken between 1996 and 2000. Samples 5 through 8 are used later to illustrate the sensitivity of the results to the observation locations. All samples except sample 2 were taken before implementation of the remediation scheme.

3.4. Results

[36] For each observation, we ran two simulations of (2), one for location probability and one for travel time probability, and we used the results in (3) and (4) to obtain the single-observation backward location and travel time PDFs, respectively. We then used (9) and (10) to obtain the multiple-observation backward location and travel time PDFs, respectively. In the backward simulations, the observations are treated as instantaneous sources in the adjoint equation, distributed over the cell or cells that contain the well screen. General information about the numerical implementation of the backward probability model is described by *Neupauer and Wilson* [2004a]. Since separate phase TCE is more dense than water, we assumed that upon entering the aquifer, the TCE was distributed vertically over the aquifer depth. In other words, we assumed that the source is distributed vertically in the aquifer; therefore we present our results as vertically integrated probability density functions.

3.4.1. Backward Location Probability Results

[37] The vertically integrated aqueous phase backward location probability density functions for the four samples on 1 January 1962, the approximate start of operations at the BOMARC Missile Site, are shown in Figures 5a–5d. These distributions represent the probability that the observed contaminant particle was in the aqueous phase at location (x_1, x_2) at any depth. The sorbed phase location probability density functions (not shown) have the same shape as these, but are scaled by $R - 1 = 0.56$.

[38] The results show that the contaminant particle observed at sample 4 is unlikely to have been near either of the suspected sources in 1962. The peak value of the PDF is more than two orders of magnitude larger than the value at CS-22 and more than four orders of magnitude larger than the value at BOMARC. Because the value of the PDF is so low at these locations, the contamination observed at sample 4 is likely to have originated from another source farther to the south. This conclusion is based on the assumption that the model is properly calibrated and the conceptual model is appropriate. Recall that sample 4 had the highest concentration of all the samples but was taken from the leading edge of the plume, an additional indication that another source of contamination nearer to sample 4 is likely.

[39] The results for the remaining samples (samples 1–3) show that the observed contaminant particles are likely to have been near the suspected sources in 1962, although the spread of the distributions is too wide to identify any particular location as the most likely source location. For each of these three samples, the most likely position of the observed contaminant particles in 1962 is downgradient of the BOMARC Site, indicating that the contamination might not have originated at the BOMARC Site. On the basis of the plume configuration (see Figure 3) and the facility history, it is likely that the BOMARC Site has contributed to the CS-10 plume. These results can therefore be indicating that another source of TCE is present downgradient of the BOMARC Site (possibly at CS-22) or they can be diagnostic of errors in the conceptual model. For example, the assumption that the TCE source was vertically distributed over the entire aquifer depth may be incorrect, or the source may not have been an instantaneous point source. Also, we assumed a linear equilibrium model for sorption. If sorption is rate-limited, more TCE will remain in the aqueous phase; thereby increasing the apparent solute velocity. Under this scenario, the aqueous phase backward location PDFs would have traveled farther upgradient, closer to the BOMARC Site [*Neupauer and Wilson*, 2004b].

[40] Combining the single-observation location PDFs using (9), we obtained the multiple-observation location PDFs shown in Figures 5e and 5f, which represent the likely positions of observed contamination on 1 January 1962, assuming the positions of the observed contaminant particles coincided at that time. Figure 5e includes only samples 1–3 because our single-observation results suggested that sample 4 was not likely to have originated at or near the BOMARC facility, while Figure 5f includes all four samples. Both plots show that CS-22 is a probable source of contamination, consistent with reports that waste from the BOMARC Site was disposed of near CS-22 [*AFCEE*, 2000]. Since we have already concluded that sample 4 originated from another source, the latter plot is not a meaningful representation of possible source locations. Recall that the multiple-observation location PDF is conditioned on the assumption that all of the observed particles were at the same location at the time of interest. This assumption appears to be violated for sample 4, and therefore sample 4 should not be included in the multiple-observation location PDF. Figure 5f is presented for illustration only to show how the use of additional samples changes the variance of the probability density functions. The spread (variance) of the multiple-observation PDF using all four samples (Figure 5f) is smaller than the spread of the PDF using three samples (Figure 5e), indicating that the uncertainty in the former position is reduced as the number of observations increases, regardless of the magnitude of the PDF. The spread of both multiple observation

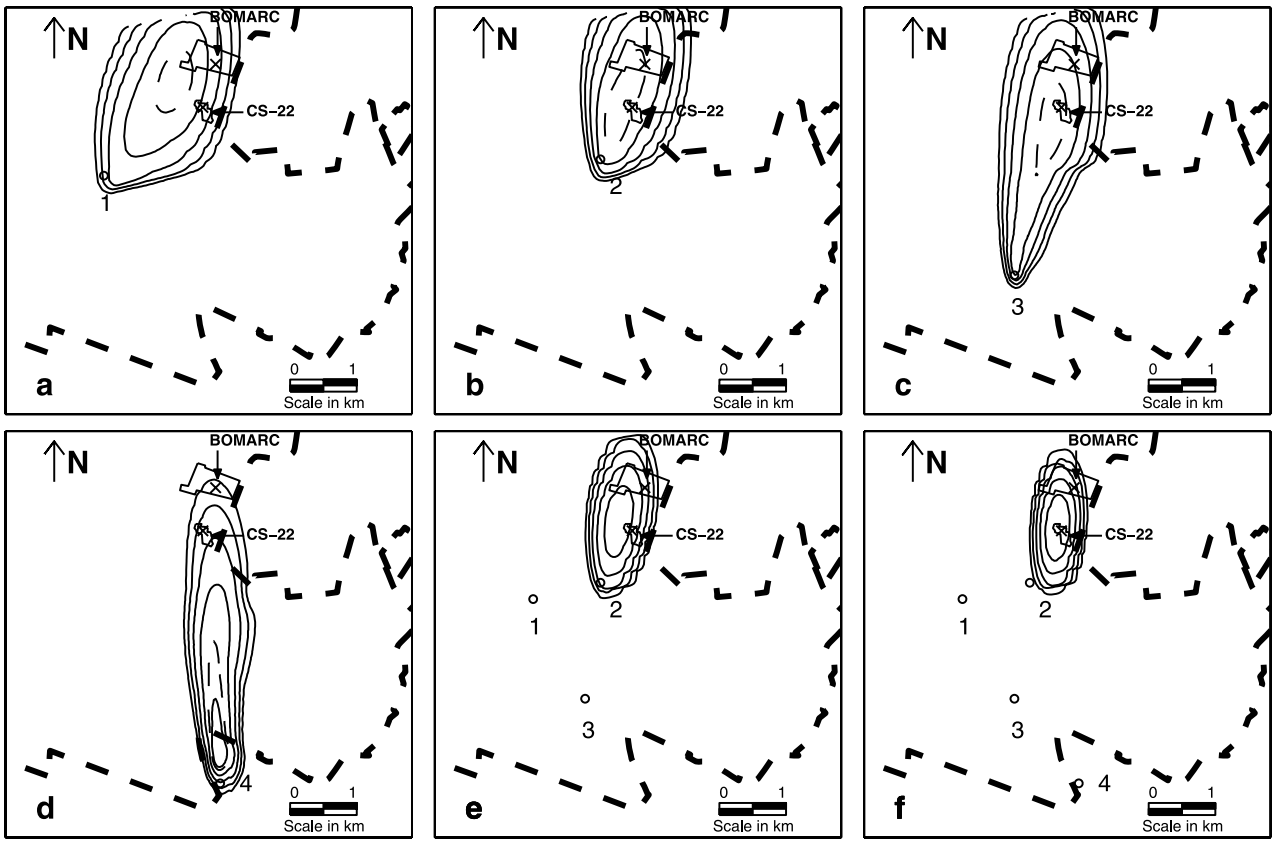

Figure 5. Vertically integrated aqueous phase backward location probability density function on 1 January 1962 for four samples (samples 1–4; Table 4). Solid contours represent values of 10^{-10} m^{-2}, 10^{-9} m^{-2}, 10^{-8} m^{-2}, 10^{-7} m^{-2}, and 10^{-6} m^{-2}. The dashed contour represents a value of 5×10^{-7} m^{-2}. (a) Sample 1, single-observation PDF; (b) sample 2, single-observation PDF; (c) sample 3, single-observation PDF; (d) sample 4, single-observation PDF; (e) samples 1-3, multiple-observation PDF; (f) samples 1–4, multiple-observation PDF. Sample locations are marked with a circle. The crosses represent the suspected source locations that are used in the travel time probability simulations.

PDFs is smaller than the spread of any single observation PDF.

3.4.2. Backward Travel Time Probability Results

[41] If the source location is known or assumed to be known, the backward travel time probability density function can be used to determine the solute travel time from the source to the observation locations. We ran backward travel time probability simulations for the four samples in Table 4 using MT3DMS. For each sample, we calculated the single-observation aqueous phase travel time PDF for releases in the BOMARC Missile Site area and the CS-22 area at locations shown by crosses in Figure 5. The source areas were each represented by one cell in the x_1,x_2 plane of the model domain, over the entire depth (21 layers). Travel time PDF is defined as a flux across a control plane in the source area, perpendicular to groundwater flow; therefore the magnitude of travel time PDF is proportional to the area of this control plane. The height of the control plane is the aquifer thickness (sum of the thicknesses of each of the 21 layers), which was 80 m (262 feet) for both source areas. The width of the control plane is the length perpendicular to flow in each layer representing the source. Since the actual source areas for the BOMARC Missile Site and CS-22 are unknown, we use a unit width for the control plane and present the results as the travel time probability density function per unit width (of the control plane).

[42] The vertically integrated aqueous phase backward travel time probability density functions for the four samples are plotted in Figures 6a–6d. For comparison, these distributions are normalized so that the total probability is unity. The sorbed phase PDFs (not shown) have the same shape but are scaled by a factor of $(R - 1)/R = 0.359$. On the plots, $\tau = 0$ corresponds to 1 July 2000. The shaded region represents the time of operation of the BOMARC Missile Site. The plots represent the most likely travel times from either the BOMARC Site or CS-22 to the sampling locations. The possible travel times to the sample locations range from 20–200+ years for the BOMARC Site, and from 12–200 years for CS-22. The long travel times are unrealistic for TCE. Sample 2 is the only sample of the four that is likely to have been at the BOMARC Site during site operations; while samples 1, 2, and 3 are likely to have been at CS-22 during operations of the BOMARC Site. These results suggest that of the two preselected sites (BOMARC and CS-22), CS-22 is more a likely source of contamination. The results could also be diagnostic of errors in the conceptual model. For sample 4, neither site appears to be a likely source, indicating that another source of TCE

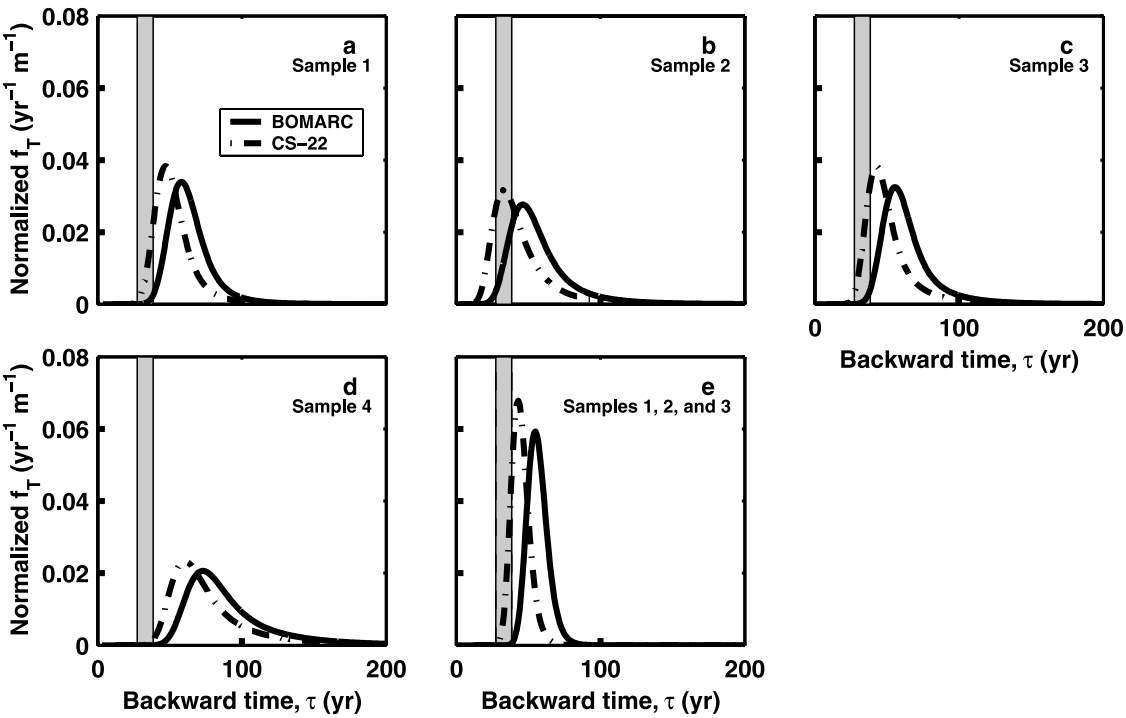

Figure 6. Normalized, vertically integrated aqueous phase backward travel time probability density functions (per unit width) from the two suspected source areas for (a) sample 1, single-observation PDF; (b) sample 2, single-observation PDF; (c) sample 3, single-observation PDF; (d) sample 4, single-observation PDF; (e) samples 1–3; multiple-observation PDF. Here $\tau = 0$ corresponds to 1 July 2000. The shaded region represents the time of operation of the BOMARC Missile Site.

near sample 4 is likely. This is consistent with the location probability results.

[43] Using the single-observation aqueous phase travel time probability density functions for samples 1–3 in (10), we calculated the multiple-observation travel time PDF, which is shown in Figure 6e. This distribution represents the time that the three observed contaminant particles were at the source location, assuming that they were all present at the same location at the same time. We did not include sample 4 because we have already concluded that it came from a different source. If the contaminant particles coexisted at the BOMARC Site, they are most likely to have been there prior to the start of operations. If they had coexisted at CS-22, they could have been there during facility operations. These results do not eliminate BOMARC as a possible source; if the source release occurred over an extended period of time, it is likely that the four observed contaminant particles did not coexist at either location, a situation that cannot be evaluated with these results. As mentioned before, errors in the conceptual model, such as the use of an equilibrium sorption model or the assumption of vertical distribution of TCE, can also affect the results.

4. Discussion

[44] The backward location probability density functions developed in this paper are a measure of the "presence" of a contaminant particle. The contaminant particle is present with certainty at the observation location and time, therefore the probability is unity that the particle exists at that location and time. This is modeled as a Dirac delta function load in the governing equation. At earlier times (later backward times), the probability density function represents the possible former positions of the observed particle. Since there are many locations where the particle could have been, the value of the PDF at any point is less than unity. This spreading out of probability density function is caused by dispersion, similar to the spreading of a unit point source in a forward model. In a forward simulation in which the source mass of a point source is unknown, the source can be modeled as a unit source and a plume representing the future contaminant distribution can be generated. If the model is linear (as it is in our case), the resulting contaminant plume can be scaled by the source strength, if it is known. Regardless of the source mass, the highest density of contamination will always be at the same location; therefore the actual magnitude is not needed to determine the future position of the contaminant. The concept is the same for backward PDFs, except that we are looking at the former position of the contamination. The effect of dispersion in the backward model is essentially the same as the effect of dispersion in the forward model.

[45] The simulation time of the backward model is proportional to the number of observations used in the model; therefore using a large number of observations may be computationally prohibitive. If a large number of observations is available, the user may choose to use only a subset of the observations, as we did in the MMR demonstration. If the complete extent of the plume is known, the observations used in the backward model should be spread throughout the plume to take full advantage of all available information. This can be compared to using multiple simulations of a forward model to identify the source location,

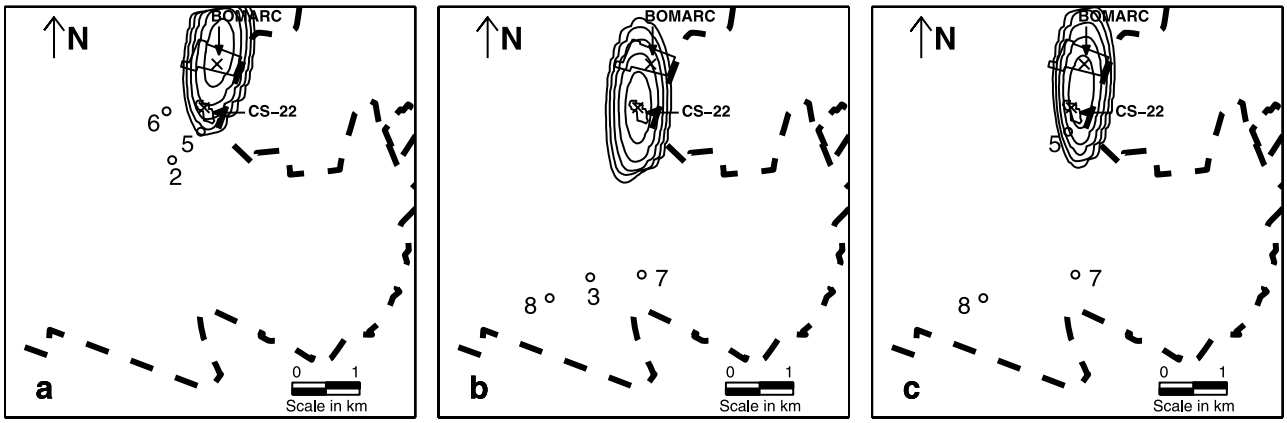

Figure 7. Vertically integrated aqueous phase backward location probability density function on 1 January 1962 for three samples. Contours represent values of 10^{-10} m^{-2}, 10^{-9} m^{-2}, 10^{-8} m^{-2}, 10^{-7} m^{-2}, and 10^{-6} m^{-2}. (a) Observations from the trailing edge of the plume, (b) observations from the leading edge of the plume, and (c) observations from both the leading and trailing edges of the plume. Sample locations are marked with a circle, and sampling times are given in Table 4.

in which the simulated plume would be compared to the entire set of observations, and the source location would be modified until a reasonable match was found. Since backward probability is a measure of the "presence" of contamination, the model gives equal weight to all observations, regardless of the concentration. The user may decide to use only observations which measured concentration values above some threshold. At a minimum, the detection limit is a reasonable threshold value.

[46] If only a few observations of contamination are available, they all should be used in the backward model. As shown in Figure 7, the position of the observations within the plume affects the likely source locations. Figure 7 shows three examples of multiple-observation location PDFs that are obtained from different combinations of three observations taken over a 2- to 4-year period, depending on the scenario (see Figure 7 and Table 4). For samples taken from the trailing edge of the plume (Figure 7a), the resulting backward location PDF identifies BOMARC or the area upgradient of it as the likely source location. For samples taken from the leading edge of the plume (Figure 7b) the resulting backward location PDF identifies CS-22 and the surrounding area as the likely source location. For samples taken from both the leading and trailing edges of the plume (Figure 7c) the backward location PDF identifies the area between BOMARC and CS-22 as the likely source location. If observations are available from only one portion of the plume, the PDF may not identify the true source location. It is not a shortcoming of the modeling approach, but a artifact of the lack of information.

[47] This method can be improved by conditioning the probability density functions on the measured concentration values. When multiple observations of contamination are made, the relative concentrations of the multiple samples provide additional information about the source location. For example, if two samples with concentrations of 1000 mg/L and 1 mg/L are taken at different locations, the source is more likely to be in the upgradient direction along a flow line passing through the location of the 1000 mg/L sample than along a flow line through the 1 mg/L sample location. An obvious first attempt at conditioning would be to weight each PDF by the sampled concentration value at that observation, which would lead to a weighted N-observation location PDF (adapted from (9)) of

$$f_{\mathbf{X}}(\mathbf{x};\tau,\{\mathbf{x}_w\},\{\tau_w\}) = \frac{\prod_{i=1}^{N}\hat{C}_i f_{\mathbf{X}}(\mathbf{x};\tau,\mathbf{x}_{wi},\tau_{wi})}{\int\prod_{i=1}^{N}\hat{C}_i f_{\mathbf{X}}(\mathbf{x};\tau,\mathbf{x}_{wi},\tau_{wi})\,d\mathbf{x}}, \qquad (11)$$

where $\hat{C}_i$ is the measured concentration at the ith observation. The numerator and denominator can both be separated into two products as

$$f_{\mathbf{X}}(\mathbf{x};\tau,\{\mathbf{x}_w\},\{\tau_w\}) = \frac{\left[\prod_{i=1}^{N}\hat{C}_i\right]\left[\prod_{i=1}^{N}f_{\mathbf{X}}(\mathbf{x};\tau,\mathbf{x}_{wi},\tau_{wi})\right]}{\int\left[\prod_{i=1}^{N}\hat{C}_i\right]\left[\prod_{i=1}^{N}f_{\mathbf{X}}(\mathbf{x};\tau,\mathbf{x}_{wi},\tau_{wi})\right]d\mathbf{x}}. \qquad (12)$$

The first product in the denominator can be taken outside the integral because it is independent of $\mathbf{x}$, and it therefore cancels with the first product in the numerator, eventually leading back to the original expression (9) for the N-observation location PDF. This simple example shows that conditioning on measured concentration values is not a straightforward extension of the approach presented here. Conditioning the backward PDFs on measured concentrations is the subject of a future paper.

5. Conclusions

[48] If contamination is observed in an aquifer, but the source of contamination is unknown, backward location and travel time probability density functions can be used to identify the former locations of the observed contamination. The backward probability model has been developed for a single observation of contamination [*Neupauer and Wilson*, 1999, 2001, 2002]. In most practical situations, contamination is observed at more than one location or time. In this paper, we developed the backward probability model for multiple observations of contamination, assuming that all of the observed contaminant particles come from the same instantaneous point source. Unlike single-observation probability density functions, which for location PDF defines any former location of the observation, these multiple-

observation PDFs are limited to source identification. The multiple-observation densities are related to the single-observation probability density functions for each of the observations through relationships based on Bayes' theorem. Using a simple, hypothetical example, we showed that the variances of the multiple-observation PDFs are smaller than the variances of the single-observation PDFs, leading to an improved characterization of the source of contamination. In general, to calculate a multiple-observation PDF, it is necessary to run one simulation of the backward probability model for each observation that is used in the backward model. Thus the procedure may become computationally inefficient if a large number of observations are considered. Even if a small subset of the observations is considered, backward model results can reveal important information about the source or former position of contamination, and the computational burden remains low. This was demonstrated in our field application at the Massachusetts Military Reservation (MMR).

[49] We demonstrated the multiple-observation backward probability model for a trichloroethylene plume at MMR to identify possible sources of contamination. Two suspected contamination sources are the BOMARC Site, a former missile site that is presently used for maintenance and storage of vehicles, and CS-22, an area where waste from the BOMARC facility was reportedly disposed of. Using four TCE samples distributed throughout the plume, we found that BOMARC and CS-22 are possible sources of some of the contamination; however CS-22 is more likely. Although our model results show a low probability that the BOMARC site is a source of contamination, these results may also be diagnostic of errors in the conceptual model, such as an incorrect sorption model. Assuming that the model is properly calibrated and that the conceptual model is correct, the results also indicated that another source of TCE near the southern area of the plume is likely.

[50] The MMR model results were obtained with only eight simulations of the backward model: one location probability simulation and one travel time probability simulation for each of the four observations. Similar information could have been obtained from forward modeling if we had selected many possible contamination sources and had run one simulation for each possible source. Many more simulations would have been required, however; therefore the backward probability model was more efficient.

[51] The quality of source information revealed by the backward probability model depends on the number, location, and timing of the observations. Extending the model to account for the values of observed concentration should reveal even more information. However, such an extension is not trivial.

[52] **Acknowledgments.** This research was supported in part by the Geophysical Research Center at New Mexico Tech and in part by the Environmental Protection Agency's STAR Fellowship program under Fellowship No. U-915324-01-0. This work has not been subjected to the EPA's peer and administrative review and therefore may not necessarily reflect the views of the Agency and no official endorsement should be inferred. The authors are grateful for the contributions of Allan Gutjahr in the early stages of development of the multiple-observation probability model. Data for the CS-10 TCE plume at MMR was provided by Sarah Stuart of Jacobs Engineering Group Inc. at Otis Air National Guard Base. Spence Smith of the Massachusetts Military Reservation provided information on the TCE contamination and remediation. Chunmiao Zheng of the University of Alabama provided his flow and transport model of the CS-10 TCE plume at MMR.

References

Air Force Center for Environmental Excellence (AFCEE) (1998), Chemical Spill 10 (CS-10) source and groundwater plume update, *Fact Sheet 98-13*, Otis Air Natl. Guard Base, Mass., July. (Available at http://www.mmr.org/cleanup/index.htm)

Air Force Center for Environmental Excellence (AFCEE) (1999), Chemical Spill 10 (CS-10) source and plume update, *Fact Sheet 99-08*, Otis Air Natl. Guard Base, Mass., Sept. (Available at http://www.mmr.org/cleanup/index.htm)

Air Force Center for Environmental Excellence (AFCEE) (2000), Air Force will conduct site investigations (SI) for the Chemical Spill-22 (CS-22), Coast Guard Chemical Spill-8 (CS-8 [CG]) and Chemical Spill-18 (CS-18) Sites, *News Release 2000-51*, Otis Air Natl. Guard Base, Mass., 26 Sept. (Available at http://www.mmr.org/cleanup/index.htm)

Chin, D. A., and P. V. K. Chittaluru (1994), Risk management in wellhead protection, *J. Water Resour. Plann. Manage.*, *120*(3), 294–315.

Dagan, G. (1987), Theory of solute transport by groundwater, *Annu. Rev. Fluid Mech.*, *19*, 183–215.

Dagan, G. (1990), Transport in heterogeneous porous formations: Spatial moments, ergodicity, and effective dispersion, *Water Resour. Res.*, *26*(6), 1281–1290.

Dagan, G. (1991), Dispersion of a passive solute in non-ergodic transport by steady velocity fields in heterogeneous formation, *J. Fluid Mech.*, *233*, 197–210.

Fogg, G. E., E. M. LaBolle, and G. S. Weissmann (1999), Groundwater vulnerability assessment: Hydrogeologic perspective and example from Salinas Valley, California, in *Assessment of Non-point Source Pollution in the Vadose Zone*, *Geophys. Monogr. Ser.*, vol. 108, pp. 45–61, AGU, Washington, D. C.

Frind, E. O., D. S. Muhammad, and J. W. Molson (2002), Delineation of three-dimensional well capture zones for complex multi-aquifer systems, *Ground Water*, *40*(6), 586–598.

Harbaugh, A. W., and M. G. McDonald (1996), User's documentation for MODFLOW-96, an update to the U.S. Geological Survey modular finite-difference ground-water flow model, *U.S. Geol. Surv. Open File, 96-485*.

Kitanidis, P. K. (1988), Prediction by the method of moments of transport in a heterogeneous formation, *J. Hydrol.*, *102*, 453–473.

Michalak, A. M., and P. K. Kitanidis (2004), Estimation of historical groundwater contamination distribution using the adjoint state method applied to geostatistical inverse modeling, *Water Resour. Res.*, *40*, W08302, doi:10.1029/2004WR003214.

Neupauer, R. M., and J. L. Wilson (1999), Adjoint method for obtaining backward-in-time location and travel time probabilities of a conservative ground-water contaminant, *Water Resour. Res.*, *35*(11), 3389–3398.

Neupauer, R. M., and J. L. Wilson (2001), Adjoint-derived location and travel time probabilities in a multi-dimensional groundwater flow system, *Water Resour. Res.*, *37*(6), 1657–1668.

Neupauer, R. M., and J. L. Wilson (2002), Backward probabilistic model of groundwater contamination in non-uniform and transient flow, *Adv. Water Resour.*, *25*(7), 733–746.

Neupauer, R. M., and J. L. Wilson (2003), Backward location and travel time probabilities for a decaying contaminant in an aquifer, *J. Contam. Hydrol.*, *66*(1–2), 39–58.

Neupauer, R. M., and J. L. Wilson (2004a), Numerical implementation of a backward probability model of groundwater contamination, *Ground Water*, *42*(2), 175–189.

Neupauer, R. M., and J. L. Wilson (2004b), Forward and backward location probabilities for a sorbing solute in groundwater, *Adv. Water Resour.*, *27*(7), 689–705.

Rajaram, H., and L. W. Gelhar (1993a), Plume scale-dependent dispersion in heterogeneous aquifers: 1. Lagrangian analysis in a stratified aquifer, *Water Resour. Res.*, *29*(9), 3249–3260.

Rajaram, H., and L. W. Gelhar (1993b), Plume scale-dependent dispersion in heterogeneous aquifers: 2. Eulerian analysis and three-dimensional aquifers, *Water Resour. Res.*, *29*(9), 3261–3276.

Saffman, P. G. (1959), A theory of dispersion in a porous medium, *J. Fluid Mech.*, *3*(6), 321–349.

Salandin, P., A. Rinaldo, and G. Dagan (1991), A note on transport in stratified formations by flow tilted with respect to bedding, *Water Resour. Res.*, *27*(11), 3009–3017.

Taylor, G. I. (1921), Diffusion by continuous movements, *Proc. London Math. Soc.*, *20*, 196–212.

Uffink, G. J. M. (1989), Application of Kolmogorov's backward equation in random walk simulations of groundwater contaminant transport, in *Contaminant Transport in Groundwater*, edited by H. E. Kobus and W. Kinzelbach, pp. 283–289, A. A. Balkema, Brookfield, Vt.

U.S. Environmental Protection Agency (USEPA) (1991), National priorities list sites: Massachusetts, *Publ. 92005-722A*, Off. of Emergency and Remedial Response, Washington, D. C., Sept.

Weissmann, G. S., Y. Zhang, E. M. LaBolle, and G. E. Fogg (2002), Dispersion of groundwater age in an alluvial aquifer system, *Water Resour. Res.*, *38*(10), 1198, doi:10.1029/2001WR000907.

Zhang, Y.-K., D. Zhang, and J. Lin (1996), Nonergodic solute transport in three-dimensional heterogeneous isotropic aquifers, *Water Resour. Res.*, *32*(9), 2955–2963.

Zheng, C., and P. P. Wang (1999), MT3DMS: Documentation and user's guide, *Rep. SERDP-99*, U.S. Army Corps of Engineers, Washington, D. C., Nov.

Zheng, C., and P. P. Wang (2002), A field demonstration of the simulation-optimization approach for remediation system design, *Ground Water*, *40*(3), 258–265.

R. M. Neupauer, Department of Civil, Environmental and Architectural Engineering, University of Colorado, 1111 Engineering Drive, Boulder, CO 80309, USA. (neupauer@colorado.edu)

J. L. Wilson, Department of Earth and Environmental Science, New Mexico Institute of Mining and Technology, 801 Leroy Place, Socorro, NM 87801, USA. (jwilson@nmt.edu)